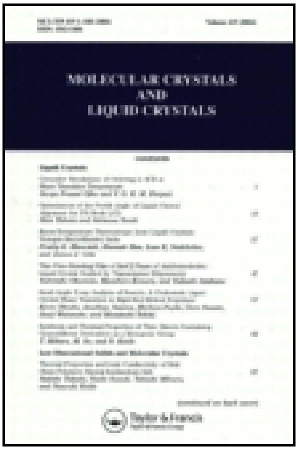

Molecular Crystals and Liquid Crystals

Publication details, including instructions for authors and subscription information:
http://www.tandfonline.com/loi/gmcl16

New 1D-Materials In The Field Of Transition Metal Chalcogenides

Jean Rouxel [a]

[a] Laboracoire de Chimie des Solides, Associé au CNRS, Université de Nances, 2, rue de la Houssinière - 44072, NANTES, CEDEX, France

Version of record first published: 20 Apr 2011.

To cite this article: Jean Rouxel (1985): New 1D-Materials In The Field Of Transition Metal Chalcogenides, Molecular Crystals and Liquid Crystals, 121:1-4, 1-13

To link to this article: http://dx.doi.org/10.1080/00268948508074823

Mol. Cryst. Liq. Cryst. 1985, Vol. 121, pp. 1-13
0026-8941/85/1214-0001/$20.00/0

NEW 1D-MATERIALS IN THE FIELD OF TRANSITION METAL CHALCOGENIDES

JEAN ROUXEL
Laboratoire de Chimie des Solides, Associé au CNRS, Université de Nantes, 2, rue de la Houssinière - 44072 NANTES CEDEX, France.

Abstract New ways have been recently opened by the chemists, on the basis of a chemical or structural expansion of the field of trichalcogenides or following the preparation of new series of derivatives. Polytypes can be found such as monoclinic-TaS_3 which presents C.D.W. type transition with possible non linear effects under low electrical field. On the other hand, varying the composition either by performing substitutions in the slabs or fibers, or by intercalating between them gave the $FeNb_3Se_{10}$ series.
However new materials are mainly represented by the blue bronzes $K_{0.30}MoO_3$ and $Rb_{0.30}MoO_3$, and by tetrachalcogenides of niobium and tantalum. The present paper will be essentially devoted to the last type of compounds. With a general formulation $(MY_4)_nX$ where M = Nb, Ta ; Y = S, Se ; X = I, Br, Cl and n = 3, 4, 2, 10/3 etc... they represent a large class of materials. The structure is based on (MY_4) chains consisting of a metallic chain enclosed in a chalcogen framework built up by rectangular antiprisms of S-S or Se-Se pairs. The MY_4 chains are parallel and separated by halogen columns. In the metallic chain variable bond lengths alternate generating a superstructure commensurate with the halogen sublattice. Some of these derivatives are very promising compounds as far as C.D.W. depinning is concerned. This is the case of $(NbSe_4)_{10/3}I$ and of $(TaSe_4)_2I$. The latter reproduces most of the exciting properties of $NbSe_3$ (particularly depinning of C.D.W. and periodic noise).

Up to now niobium triselenide [1] represents one of the most fascinating among one-dimensional materials. It shows two charge density waves occurring respectively at 145 and 59 K and leading to super structures non commensurate with the underlying sublattice. The most striking properties of $NbSe_3$ are in fact the non linear transport properties under low electrical fields and the behaviour at microwaves frequencies which are observed below the two independent C.D.W. transitions. These properties have been associated to a motion of the C.D.Ws which were initially pinned to the lattice. A sufficient electric field is necessary to overcome the pinning energy which depends on various factors such as interchain coupling, chemical impurities, gap to commensurability with the underlying lattice. A better understanding of these phenomena largely relies on chemists who can act upon these various factors and we tried to give some answers through :

(i) the search of polytypes, as illustrated by TaS_3 [2,3,4]
(ii) the effects of doping which leads to the MNb_3Se_{10} series [5]
(iii) the search of materials more 1D in character (TaS_3 again)
(iv) the preparation of new series, as discussed in this paper.

NEW SERIES OF C.D.W. COMPOUNDS : THE $(MX_4)_nY$ DERIVATIVES (M = Nb, Ta ; X = S, Se ; Y = Cl, Br, I).

In the search of new interesting materials the consideration of anionic pairs should receive a large attention. Indeed the presence of anionic pairs in trichalcogenides makes them different from dichalcogenides. Formally NbX_3 can be formulated as $Nb^{4+}(X_2)^{2-}X^{2-}$. The metal configuration (d^1) accounts for the metallic properties of the chains. It may lead also to the formation of metal-metal pairs with correlatively a semi-conducting behavior as observed in NbS_3. However things are complicated by the fact that the anionic pairs exhibit various bond lengths, which allows trichalcogenides to be classified as a function of the number n of different $[MX]_3$ chains ($ZrSe_3$ n = 1, $TaSe_3$ n = 2, $NbSe_3$ n = 3). In these compounds $[X_2]^{2-}$ anionic pairs clearly behave as "electron reservoirs". Depending upon their lengths they give different electrical properties to the metallic chain (Nb or Ta).

In the mineral VS_4 two anionic pairs, and not only one like in trichalcogenides, are present in the structure. A d^1-d^1 pairing gives a diamagnetic semi-conducting behaviour to this compound. We did not succeed when trying to prepare NbX_4 or TaX_4 homologues. But adding an halogen a complete series of new materials was found with general formulation $(MX_4)_nY$.

The common structural model can be illustrated by considering $(NbSe_4)_3I$ [6]. Single needle-shaped crystals of this phase were obtained by mixing the starting elements in an evacuated and sealed glass tube at temperatures ranging from 400 to 550°C. $(NbSe_4)_3I$ crystallizes with tetragonal symmetry, space group P4/mnc. Unit cell parameters are a = 9.489(1) and c = 19.13(3) Å. The structure (Figure 1) is composed of $[NbSe_4]$ chains and iodine columns which are both parallel to the c axis. Two niobium atoms having the same z value, but belonging to different chains are 6.70 Å apart. Along the chains six niobium atoms are located within one c parameter. Two different Nb-Nb distances (3.06 and 3.25 Å)

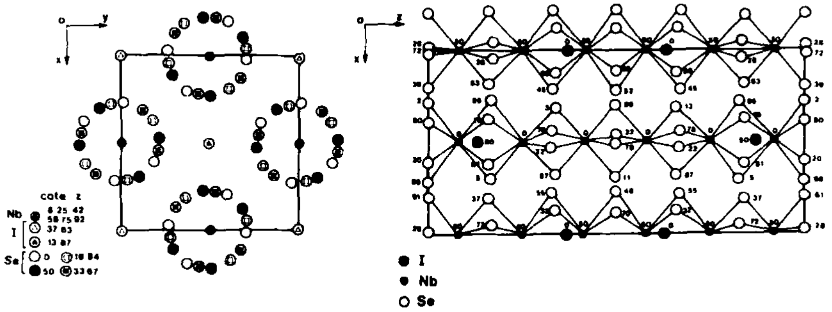

FIGURE 1 - $(NbSe_4)_3I$

occur along the axis according to the sequence of two longer distances followed by one short Nb-Nb bond. The niobium coordination is a rectangular antiprism composed of four $(Se_2)^{2-}$ pairs. The dimensions of each rectangle are about 3.5 and 2.35 Å. The latter value corresponding to the typical $(Se_2)^{2-}$ pairing. The antiprisms are stacked along the c axis in a screw-like arrangement. The iodine atoms are located between the $NbSe_4$ chains.

The metal-metal sequences change in the various compounds[7] as a function of the amount of counter ion (Table I). The two sublattices, metal chains and halogen columns remain commensurate to each other.

TABLE I Various metal-metal sequences in the $(MX_4)_nY$ compounds.

Compound	M-M sequence	ρ_{Rt} (Ω.cm)	E(eV)
$(NbSe_4)_3I$	$— \mathrm{Nb} \overset{3.25}{——} \mathrm{Nb} \overset{3.25}{——} \mathrm{Nb} \overset{3.06}{——} \mathrm{Nb} —$	1	0.19 at RT
$(NbSe_4)_{3.33}I$	$— \mathrm{Nb} \overset{3.17}{——} \mathrm{Nb} \overset{3.23}{——} \mathrm{Nb} \overset{3.15}{——} \mathrm{Nb} \overset{3.23}{——} \mathrm{Nb} —$	10^{-2}	0.13
$(TaSe_4)_2I$	$— \mathrm{Ta} \overset{3.206}{——} \mathrm{Ta} \overset{3.206}{——} \mathrm{Ta} —$	1.5 10^{-3}	0.25
$(TaSe_4)_3I$	(same sequence as for $(NbSe_4)_3I$)	0.2	?
$(NbSe_4)_4Br$	$— \mathrm{Nb} \overset{3.15}{——} \mathrm{Nb} \overset{3.15}{——} \mathrm{Nb} \overset{3.15}{——} \mathrm{Nb} \overset{3.45}{——} \mathrm{Nb} —$	50	0.36
$(NbSe_4)_3Br$	?	8	0.25
$(TaSe_4)_4Br$	?	3.5	0.18

When the metal-metal distances are equal a high conductivity state is observed at room temperature. That is the case of $(TaSe_4)_2I$ with a room resistivity of 1.5×10^{-3} Ω .cm. As shown in figure 2, this compound undergoes a transition towards a semiconducting state at 263 K [8-9]. The transition has a C.D.W. origin and superlattice spots have been observed by electron diffraction studies [10-11]. If the q vector is taken as the vector connecting the satellite spot to the nearest Bragg spot its c* component is 0.057 ± 0.002 c*, which would lead to a Fermi wave vector k_F = 0.028 c* in consistent with the metallic properties of the material because it involves that the Fermi Level is at the bottom of the conduction band. But on the other hand we can consider that the q vector connects the satellite spot to a non nearest Bragg spot which leads to a c* component of 0.94 c* (second nearest Bragg spot). This reminds us of a similar situation observed in 1T TaS_2 [12]. The value of the q vector will be confirmed by band structure calculations (see below).

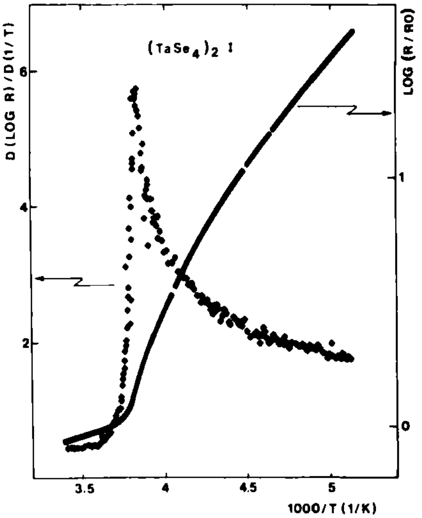

FIGURE 2 - Electrical behaviour of $(TaSe_4)_2I$.

$(TaSe_4)_2I$ presents non linear properties above a threshold field [8-9-13] as observed for $NbSe_3$ and TaS_3. Figure 3 shows some typical non linear differential resistance curves as a function of the applied current for different temperatures. The threshold electric field is reached when dV/dI starts to decrease (E_c = R × I_c/l where l is the length of the sample). Above the threshold field a time dependent voltage is also manifested (Figure 4) under the form of a broad band noise and a periodic signal which can be decomposed in a fundamental and its harmonics. The peaks are displaced towards higher frequencies if the applied field increases. Non-linearity in transport properties is assumed to be the consequence of the motion of the C.D.W. in the periodic pinning potential created by impurities. The threshold field is the field for which the electric force applied on the C.D.W. overcomes the pinning forces.

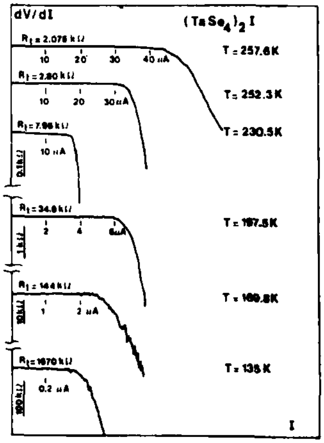

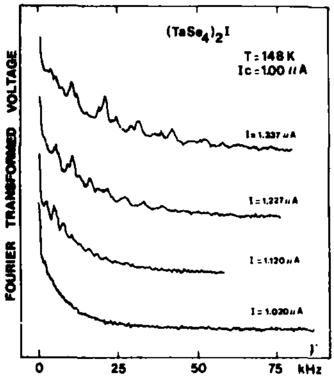

Figure 3 - Non linear effects in $(TaSe_4)_2I$.

Figure 4 - Fourier analysis of the voltage accross the voltage at 148 K.

In the non linear regime the current is the summ of an ohmic contribution and a contribution due to the moving of the C.D.W. with velocity v :

$$J = J_{ohm} + n\ e\ v,$$

where n e is the electronic concentration in the bands affected by the C.D.W. gap. The velocity v can be written as $v = \lambda \nu$ where ν is the fundamental frequency measured in the Fourier analysis of the voltage and $\lambda = 2\pi/q$. Consequently this should lead to a linear relationship between $J_{C.D.W.} = n\ e\ v$ and ν :

$$J_{C.D.W.} = (n\ e\ \lambda)\ \nu$$

Figure 5 shows the linear relationship which is observed between ν and $J_{C.D.W.}$ in the case of $(TaSe_4)_2I$. An other interesting compound in the series is $(NbSe_4)_3I$ although its structure is more complex. $(NbSe_4)_{10/3}I$ has the same a parameter (tetragonal symmetry) but the c parameter is 10/6 times that of $(NbSe_4)_3I$. Ten niobium atoms are distributed along the metallic chain according to the following bond sequence :

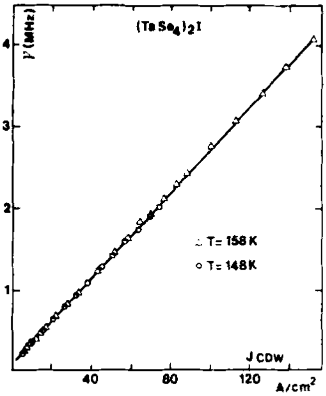

FIGURE 5 - The fundamental frequency as a function of J_{CDW} in $(TaSe_4)_2I$ at 148 and 158 K.

$$\text{— Nb} \overset{3.232}{\text{———}} \text{Nb} \overset{3.171}{\text{———}} \text{Nb} \overset{3.232}{\text{———}} \text{Nb} \overset{3.150}{\text{———}} \text{Nb}$$

0 Z values 1/4 1/2

The Se_4 rectangular antiprisms are unchanged but the iodine atoms do not show the same distribution within all the channels like in $(NbSe_4)_3I$ or $(TaSe_4)_2I$. We have to distinguish between two types of channels (i) one along the 00z axis which is occupied by four iodine atoms (ii) the other one along the ½,½,z axis which is concerned by only two iodine atoms. In the first case iodine is closely bonded to four selenium atoms (I-4Se = 3.272 Å) while in the second case it is rather weakly bonded to eight selenium atoms (I-8Se = 3.469 Å) in a square antiprismatic arrangement.

The room temperature resistivity along the needle axis is 1.5×10^{-2} Ω.cm. A phase transition is observed at 285 K as it is clearly shown (Figure 6) by a peak in the logarithmic derivative curve d Log(R/R_0)/d(1/T). The Peierls origin is demonstrated by the appearance of superlattice spots in the electron diffraction pattern[10]. The q vector is (0, 0, 0.487 ±0.002 c*) and the Fermi wave vector is 0.243 c*.

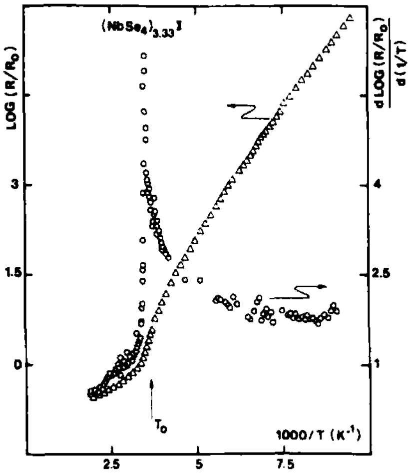

Figure 6 - Variation of the resistance of $(NbSe_4)_3I$ (after ref. 14).

For any temperature below the transition, non linear transport properties can once more be observed if the applied field exceeds a threshold value. An interesting point is that an hysteresis phenomena takes place in the 285-220 temperature range (Figure 7). This type of memory effect, also observed in orthorhombic TaS_3 [15] and in the blue bronzes $K_{0.30}MoO_3$ [16] depends on the electrical history of the sample. It implies that probably closely related

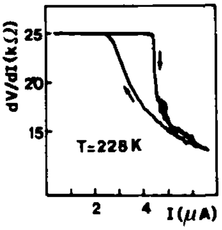

FIGURE 7 - Memory effect in $(NbSe_4)_{3.33}I$ at 228 K.

metastable states of comparable energy are concerned in pinning effects. We have a threshold field when the field is increased and a different one when it is decreased. Like in $(TaSe_4)_2I$ E_c increases approximately exponentially when the temperature is reduced below T_c. Near T_c it goes through a minimum. Below the transition the fundamental frequency of the noise spectra varies once more linearly as a function of $J_{C.D.W.}$.

$(NbSe_4)_3I$ and its homologue $(TaSe_4)_3I$ also present similar structural and electrical transitions when the temperature is decreased (Figure 8). It has not been possible to establish a C.D.W. origin of these transitions which occurr at 275 K for the niobium derivative and about 200 K for the tantalum one.

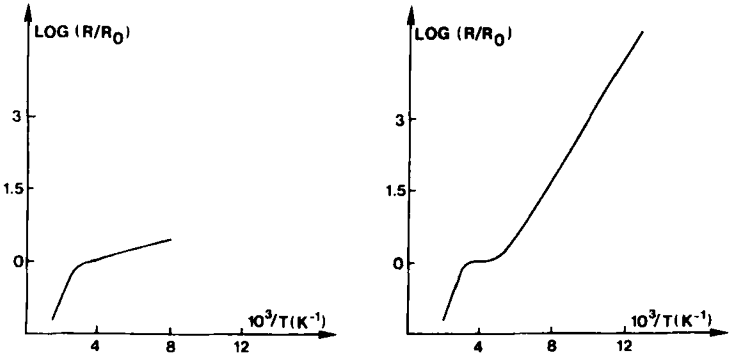

FIGURE 8 - Log R/R_0 versus $10^3/T$ for $(NbSe_4)_3I$ type I(a) and type II(b) crystals.

Electron diffraction studies [10] show that the phase transition is manifested by a change in space group with a disappearing of the glide plane n.

CONCLUSIONS AND DISCUSSION

The many $(MX_4)_nY$ phases form one of the best series to insure a progression of the C.D.Ws studies. They present all the striking properties observed in trichalcogenides but here we have a much more interesting flexibility of the systems. Interchain coupling can be change according to the size and electronegativity of the counter ion iodine, bromine or chlorine. The amount of counter-ion changes also the electronic density available along the chains and from that point of view the tetrachalcogenides are reminiscent of the Krogmann salts. They also structurally remind us some organic conductors containing iodine such as tetraselenotetracene-I_x [17].

The electronic properties of a $[MSe_4]$ chain are largely determined by the interactions of the metals dz^2 orbitals along the chain taken as the z axis of the system. This is illustrated in the resistivity values of the compounds, the highest one referring to the greatest difference between long and short M-M distances. If the role of the halogen is neglected each $[MSe_4]$ chain has an M^{4+} (d^1) metal ion at the center of every Se_8 rectangular antiprism. Iodine atoms, and other halogens too, are isolated from one another (the I-I interatomic distance is 4.76 Å in $(NbSe_4)_3I$ for example, which is very large when compared to 2.68 Å in solid I_2 and a maximum of 3.07 Å in I_3^-. Each iodine takes about one electron. Thus for $(MSe_4)_nI$ the average number of d electrons on each M would be $(n-1)/n$. The corresponding filling of the dz^2 band is $f = (n-1)/2n$ possibly leading to a distortion increasing the repeat distance by a factor $1/f$. This first approach suggests that $(NbSe_4)_3I$, $(NbSe_4)_{10/3}I$ and $(TaSe_4)_2I$ would have 1/3, 7/20, and 1/4 filled dz^2 bands respectively. As n increases the dz^2 band of $(MSe_4)_nI$ becomes closer to 1/2 filled. Vanadium tetrasulfide constitutes finally an example of the $n \to \infty$ limit. It has a 2c insulating Peierls distortion. More precisely tight-binding band structures calculations have been performed [18]. They are in rather good agreement with the observed distortions. For example the calculations on $(TaSe_4)_2I$ lead to an estimation of $2k_F = 0.88$ c* and the distortion is observed at 0.94 c* in ref. [10] and 0.91 in ref. [11].

Like transition metal trichalcogenide the $(MX_4)_nY$ phases are obtained in sealed tubes, i.e. under thermodynamic conditions that are not well defined. A small range of temperature is associated to particular starting conditions (quantities of elements, volume of the tube) in order to get a given compound. In addition the structural similarity of all the compounds with only slight changes in the iodine repartition and in the metallic sequence along the chains makes it possible to observe intergrowth phenomena. This is what was probably observed in the case of some $(NbSe_4)_3I$ crystals which present at low temperature a particular behavior (Figure 8b). The corresponding crystals cannot be distinguished by X-Ray techniques. They both present the characteristics of $(NbSe_4)_3I$. The measurements have been reproduced at least three times on different crystals of both types. Both type crystals have a room resistivity of about 1 Ω.cm. Type I behavior is characterized by a very small semi-conducting gap below 275 K. In type II crystals, after the same decrease of the gap at 275 K, the resistivity increases again at lower temperatures showing a behavior very similar to the one of $(NbSe_4)_{3.33}I$ at these tempereatures (E = 0.13 eV instead of 0.11 eV for $(NbSe_4)_{3.33}I$. This suggests that type II crystals could present microdomains of the $(NbSe_4)_{3.33}I$ composition. Without any modification of the structural framework this would essentially result in different local arrangements of iodine ions. This is an important point concerning chemistry, i.e. the first illustration of a one-dimensional phase intergrowth. On the other hand it may explain some unexpected results obtained recently in an other group [19]. It may also shed some light on the real nature of defects pinning charge density waves. As well as in trichalcogenides there is a high probability that such defects are not only represented by chemical impurities but also by chemical defects such as a local variation of the Se-Se bond lengths or structural defects due to intergrowth mechanisms.

A last point to discuss concerns the decrease of the semiconducting energy gap in both types of $(NbSe_4)_3I$ at 275 K. this unusual behavior leads to a higher conducting state when lowering the temperature. It supposes a modification of the electronic density along the chains. A reasonable explanation could be found in the formation of $(I_3)^-$ ions from isolated I^- ions along the iodine columns. This would result in a two-thirds decrease of the number of Nb^{5+} (d^0) ions along the metallic chains. An other possibility is that the structural change which is observed below the electrical transition concerns the selenium antiprisms. Anyway the transition will result in a change of the metal-metal bond length sequences. Experiments are currently underway to check these hypothesis.

REFERENCES

1. A. Meerschaut and J. Rouxel, J. Less Common Metals, 39, 197 (1975).
2. E. Bjerkelund and A. Kjekshus, Z. Anorg. Chem. B, 328, 235 (1964).
3. T. Sambongi, K. Tsutsumi, Y. Shiozaki, M. Yamamoto, K. Yamaya, Y. Abe, Sol. State Comm., 22, 729 (1977).
4. A. Meerschaut, J. Rouxel, P. Haen, P. Monceau, M. Nunez-Regueiro, J. Phys. Lett., 40, L157 (1979).
5. A. Meerschaut, P. Gressier, L. Guemas, J. Rouxel, Mat. Res. Bull., 16, 1035 (1981).
6. A. Meerschaut, P. Palvadeau and J. Rouxel, J. Solid State Chem., 20, 21 (1977).
7. P. Gressier, A. Meerschaut, L. Guemas, J. Rouxel and P. Monceau, J. Sol. State Chem., 51, 141 (1984).

8. Z.Z. Wang, M.C. Saint-Lager, P. Monceau, M. Renard, P. Gressier, A. Meerschaut, L. Guemas and J. Rouxel, Sol. State Comm., 46-4, 325 (1983).
9. M. Maki, M. Kaiser, A. Zettl and G. Grüner, Sol. State Comm., 46-7, 29 (1983).
10. C. Roucau, A. Ayroles, P. Gressier and A. Meerschaut, Journal of Physics C,
11. H. Fujishita, M. Sato and S. Hoshino, Sol. State Comm., 49-4, 313 (1984).
12. J.A. Wilson, F.J. Di Salvo and S. Mahadjan, Adv. Phys., 24, 119 (1975).
13. G. Mozurkewich, M. Maki, G. Grüner, Solid State Commun., 48(5), 453 (1983).
14. Z.Z. Wang, P. Monceau, M. Renard, P. Gressier, L. Guemas, A. Meerschaut, Sol. State Comm., 47-6, 439 (1983).
15. L. Mihaly and G. Grüner
G. Mihaly and L. Mihaly, Sol. State Comm., 48, 449 (1983).
16. J. Dumas and C. Schlenker, Proc. Int. Conf. Sapporo Japan october 1983.
17. P. Delhaes, C. Coulon, S. Flandrois, B. Hilta, C.W. Mayer, G. Riho and J. Rivory, J. Chem. Phys., 73, 1452 (1980).
18. P. Gressier, M.H. Whangbo, A. Meerschaut and J. Rouxel, Inorg. Chem., April 1984.
19. H. Fujishita, M. Sato and S. Hoshino, Sol. State Comm., 49-4, 313 (1984).